International Journal of Applied Engineering Research ISSN 0973-4562 Volume 12, Number 17 (2017) pp. 6862-6869

Structural Safety Analysis of Main Shaft for Wind Power Generators Considering Mass Effect

Jong Hun Kang
Assistant Professor, Department of Mechatronics Engineering,
Jungwon University, Munmu-ro 85, Geosan Gun, Chungbuk,, South Korea.

Orcid ID: 0000-0002-9821-7149 & Scopus Author ID: 56283063600

HyoungWoo Lee*
Assistant Professor, Department of Mechatronics Engineering,
Jungwon University, Munmu-ro 85, Geosan Gun, Chungbuk,, South Korea.
** Corresponding aurthor*

Abstract

The main shaft for wind power generators, the largest part in the nacelle, is manufactured by casting or forging. The weight of the main shaft, depending on the design, is generally 10 to 20 tons, and thus is significantly affected by the mass effect in cooling. In the present study, a cooling test was performed with a large specimen of 42CrMo4, which is often used as the material for the main shaft, to empirically obtain the hardenability from the surface. Since the hardenability is dependent on the size of the main shaft, for standardization, DEFORM and JMatPro software programs were used to predict the hardness on the cooling curve at different positions and the predicted results were compared with the experimental hardenability results. When the mass effect was considered, the strength was higher at a position closer to the surface and lower at a position closer to the core. These experimental results were expressed as a function of mechanical strength depending on the depth. An ANSYS structural analysis was performed to calculate the equivalent stress. The safety factor was compared between the case where the mass effect was considered and the case where the yield strength was constant over the entire specimen for a more accurate evaluation of the structural safety.

Keywords: Wind Turbine, Main Shaft, Mass Effect, Finite Element Analysis, Safety Factor

INTRODUCTION

The main shaft of wind power generators is the part that transmits the power of the blades to the gear box [1]. The mechanical elements for wind power generators are generally manufactured by open die forging. As shown in Figure 1, in a wind power generator, the main shaft is a core mechanical part that transmits the rotational power of the rotor hub to the gear box and it accounts for the highest weight among the individual parts for wind power generators.[1-3]

The common internal defects that have a significant effect on the quality of large-sized forgings include pores and nonmetallic inclusion defects remaining in the raw material, insufficient mechanical properties due to the mass effect of large-sized products, and folding and dimensional problems due to process design errors. Among these problems noted above, the metallic defects of forgings have been significantly improved thanks to the development of casting and forging technologies for raw materials. With regard to the mechanical properties depending on the mass effect, the hardenability has been standardized for standard specimens or specimens having a maximum thickness of 100 mm [4-6]. However, since the general diameter of the recently used main shafts for 2 MW to 4 MW wind power generators is usually Φ400 to 1000 mm, the mechanical properties in the core may not be predicted on the basis of the hardenability of the standard thickness.

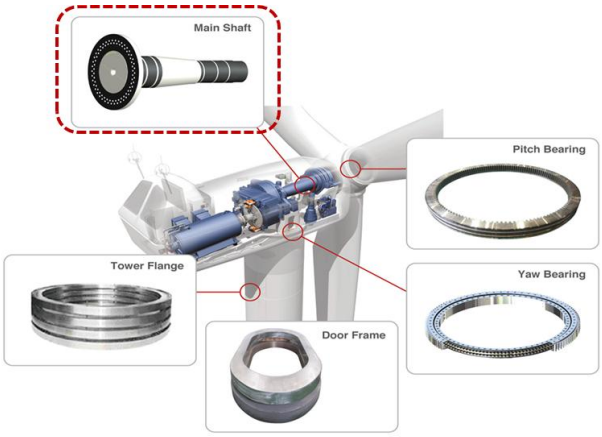

Figure 1: Main shaft of wind power generator[2]

In the present study, the hardness and the microstructure of a 400 x 400 x 400 mm specimen obtained from a forged main shaft were measured according to the Jominy test method [7] by preparing a tester that can cool one portion of the surface with water. Analytical prediction of the experimental results enables the prediction of the strength at individual positions of the heavy object. In the present study, the hardness, strength, and fraction at different positions depending on the cooling

rate were calculated by using JMatPro software, and the calculated results were compared with the experimental values.

Since the main shaft is a component on which high transmitted force is applied, torque and bending moment are usually involved. In the present study, the analysis was performed with a 5 MW shaft having an open design structure [8]. The safety factor considering the mass effect was calculated by using the analytical results.

JOMINY TEST OF LARGE-SIZED PRODUCT

The Jominy test is a representative test method for measuring the hardenability of steel. A cylindrical specimen having a diameter of 25 mm and a length of 100 mm is heated to a hardening temperature, placed vertically, and then cooled by spraying water on the bottom surface. After cooling, the hardness is measured in the length direction from the tip of the water quenching starting region, and then a hardness trend curve is plotted to obtain a hardenability curve.

While the Jominy test is a method of measuring the hardenability of steel materials, large-sized products such as the main shaft are not cooled as rapidly as the standard specimens, and the cooling rate in the core part far away from the surface is extremely slow. Hence, the variation of the hardness in a large-sized product may need to be obtained by performing the Jominy test with a specimen of an actual product size to predict the mechanical properties at individual positions through an analytical method. To perform the Jominy test with a large-sized specimen, a large-sized Jominy specimen was prepared from a normalized forging product, and a test apparatus was prepared. Table 1 shows the chemical composition of the raw alloy material.

The size of the large-sized Jominy specimen taken from a forged product having a size of Φ1188 X 1160 mm was 400 x 400 x 400 mm. One side of the specimen was cooled with water, and the other regions were air-cooled as in the general Jominy test. Figure 2 shows a schematic diagram of the test apparatus and photos showing the starting and finishing stages of the test.

Table 1: Chemical composition of Jominy test material(Wt%)

	C	Si	Mn	P	S	Cu	Ni	Cr	Mo	Al	V
Min	0.40	0.15	0.80	-	-	-	-	1.00	0.20	0.020	0.03
Max	0.43	0.35	0.90	0.025	0.030	0.30	0.25	1.20	0.30	0.035	0.08
Value	0.40	0.26	0.85	0.011	0.004	0.05	0.09	1.10	0.24	0.028	0.06

Hardness Inspection

From the specimen end-quenched in the Jominy test, three coupons were taken from the surface, 1/2R, and center of the end-quenched specimen, respectively, to analyze the hardness at different positions of the material. Figure 3 shows the positions where the coupons were taken and the obtained coupons. The size of the coupons was 30 x 30 x 400 mm, and the coupons were cut into rectangular blocks.

The C1, R1, and S1 coupons were completely transformed by the Jominy test. Since structural steel is used after quenching and tempering, the C2, R2, and S2 coupons were prepared by tempering for two hours at 580℃, which is the actual tempering temperature.

The hardness was measured with the C1, R1, and S1 coupons directly obtained from the large-sized specimen and the C2, R2, and S2 coupons that had undergone tempering at 580℃. The hardness was measured in the Rockwell hardness (HRC) scale. The measurement was performed according to the ASTM standards from the cooling position to 50 mm and in a certain interval from 50 mm to 400 mm.

(a) Normalized Forging Block

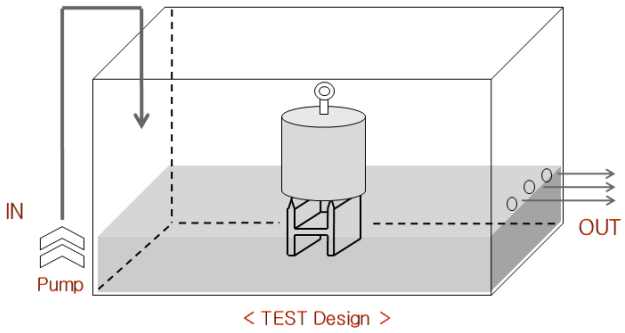

(a) test method

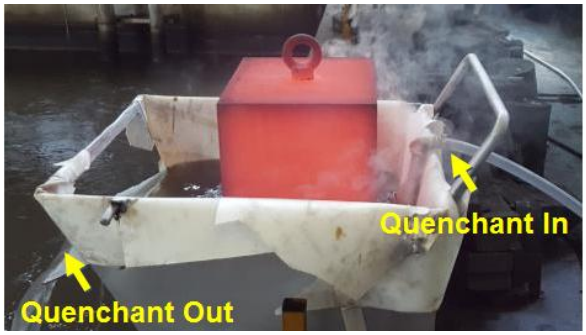

(b) Before Jominy Quenching

(c) After Jominy Quenching

Figure 2: Jominy test equipment

Since the hardness of the 30 x 30 x 400 specimen could not be measured, the specimen was 1/2 split in the length direction. Figure 3 shows the split specimen.

Figure 4 shows the measured hardness. The hardness was high from the surface to 50 mm and became constant from 100 mm.

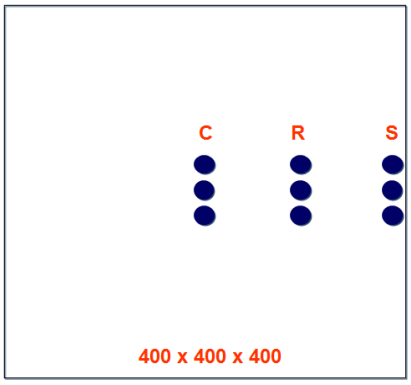

(a) test coupon location

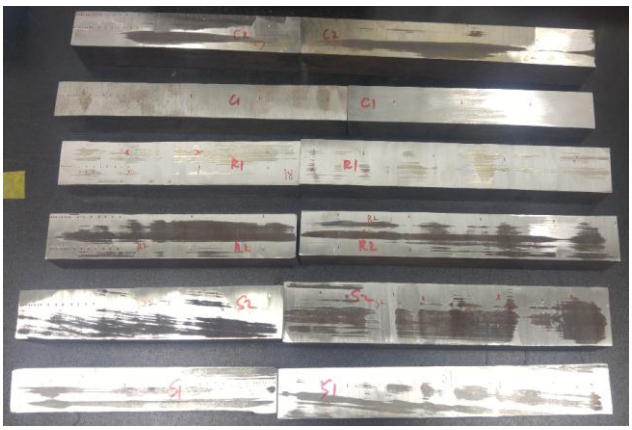

(b) test coupon

Figure 3: Hardness inspection specimens

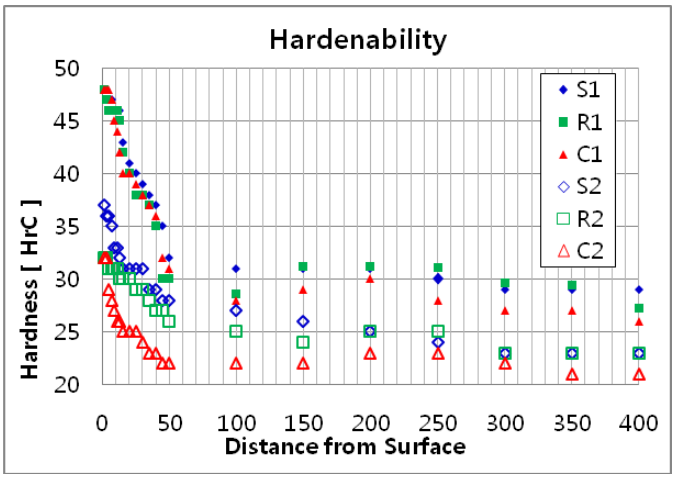

Figure 4: Hardness results of different position

The hardness was not significantly different among the C1, R1, and S1 coupons of the quenched material, but significantly different in the C2, R2, and S2 coupons of the tempered material. The hardness of the tempered material coupons was lower than that of the quenched material coupons. Smoothing to a degree found in the literature was not shown, but to the degree where the gradient of the reduction of hardness may be decreased. This difference may be because the analysis in the present study was performed with coupons taken from a large-sized specimen and thus the range of the analysis was different between the present study and the previous study. In the analysis of the coupons having a diameter of 100 mm, smoothing was verified through a comparison of C1 and C2 coupons.

Microstructure

In the 50 mm range where the hardness of the Jominy specimen was drastically changed, the microstructure was observed at the positions of 1.5 mm, 9 mm, 20 mm, 50 mm, and 400 (specimen end). According to the hardness plot, a bainite structure was expected to appear up to 50 mm and then decrease gradually, and a ferrite structure and a perlite structure were expected to appear from 50 mm.

The microstructure images showed that martensite was dominant at 1.5 mm, bainite was found at 9 mm, 20 mm, and 50 mm, and rapidly cooled ferrite and pearlite were observed at 400 mm.

The microstructure images were taken for the C, R, and S coupons, but a 200 magnification optical microscope image of the C coupon is shown in Figure 5 as a representative image.

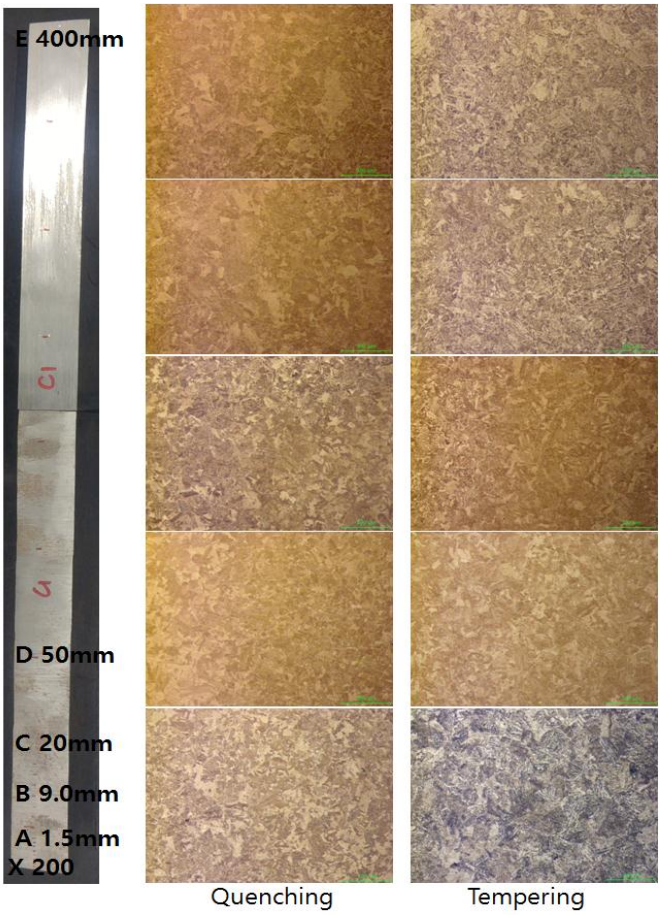

Figure 5: Positional Microstructure of C region

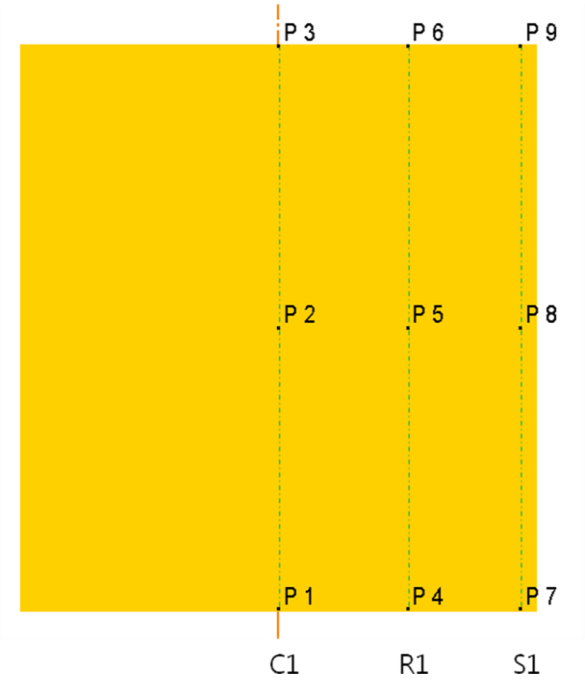

Figure 6: Temperature calculation position

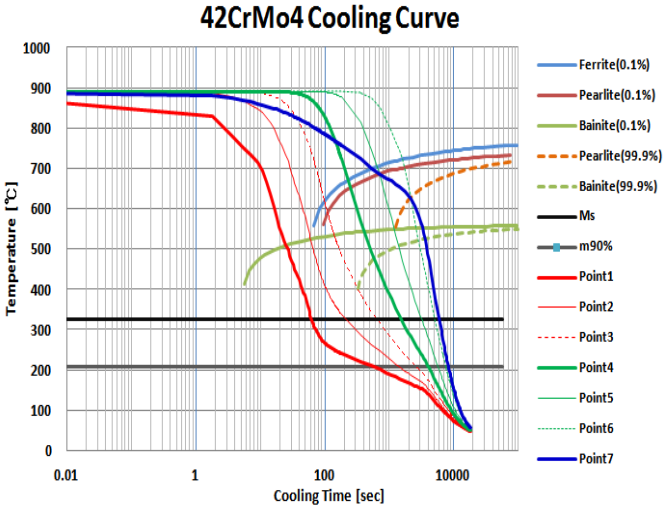

Figure 7: CCT and positional cooling curve

Hardness analysis by Jmatpro

A continuous cooling transformation (CCT) curve was generated by using JmatPro software based on the chemical composition of 42CrMo4M and the austenizing temperature. Since the Jominy test is a type of quenching test, the microstructure and the strength may be predicted by inputting the cooling curve for the measurement position. In this method, however, only the hardening strength may be predicted, because the softening by the tempering is not considered. To predict the hardness by using JmatPro software, the representative positions of the Jominy specimen were selected from the hardness measurement positions, and the cooling curve over time at each position was calculated by using the DEFORM software. The hardness, mechanical properties, and fractions of individual components were then calculated by using the Quench Property module of the JmatPro software. Figures 6 and 7 show the positions used to predict the mechanical properties and the CCT curves and the temperature variation at the individual positions.

Figure 7 shows that the cooling rate was not significantly different among the C, R, and S positions. Therefore, the hardness and the strength were calculated in the present study along the length from the surface at the C position.

Figure 7 shows that the temperature difference on the cooling surface was almost negligible, but the difference of the cooling rate was increased as the distance of the measurement position from the water cooling position was increased. The variation of the temperature over time at 1.5 mm, 9 mm, 20 mm, 50 mm, 100 mm, 200 mm, and 398.5 mm from the cooling surface at the core (C1) was calculated by using the DEFORM software, and the hardness was calculated by using the cooling curve for each position and the JmatPro software. P1 to P7 points were determined sequentially from the cooling surface, and the cooling rate over time at each of the points was plotted as shown in Figure 8.

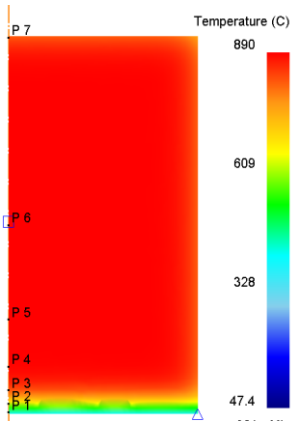

(a) Positional temperature analysis

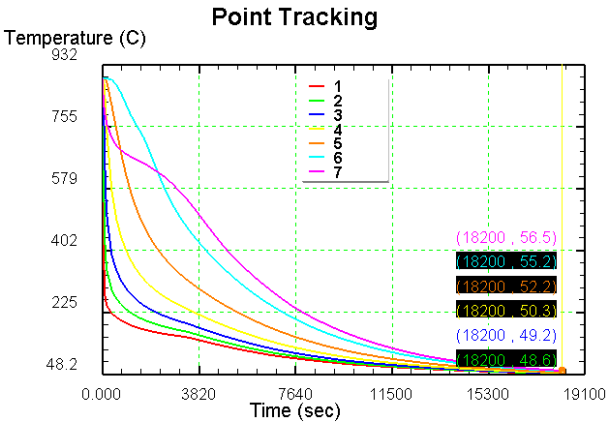

(b) Positional temperature curve

Figure 8: Temperature calculation position and temperature gradient of each

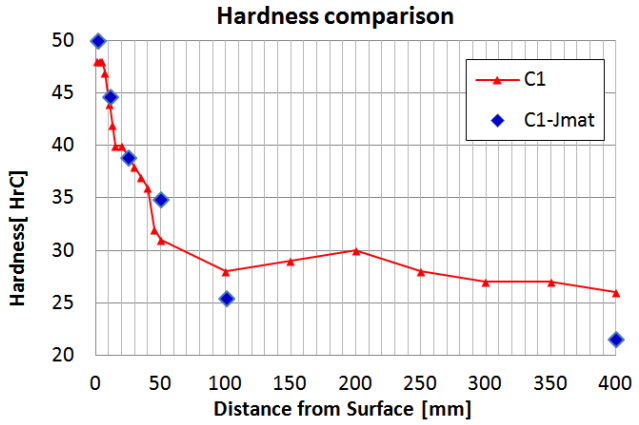

Figure 9: Hardness comparison between test and analysis

The hardness, strength, and microstructure fraction were calculated from the individual cooling curves and the CCT curve by using the Quenching Property module of the JmatPro software. Figure 9 compares the hardness measurement results from the Jominy test and the hardness calculated by the JmatPro software. Figure 10 shows the calculated microstructure fractions at 1.5 mm, 9 mm, 20 mm, 50 mm, and 400 mm, which were the positions where the optical microscope images were taken.

Figure 10 shows that bainite was dominant in the range up to 50 mm where the hardness was high. Ferrite and pearlite were found in the positions farthest from the Jominy position. The calculated phase content and the hardness distribution obtained from the JmatPro software were consistent with the hardness data and the optical microscope images obtained experimentally.

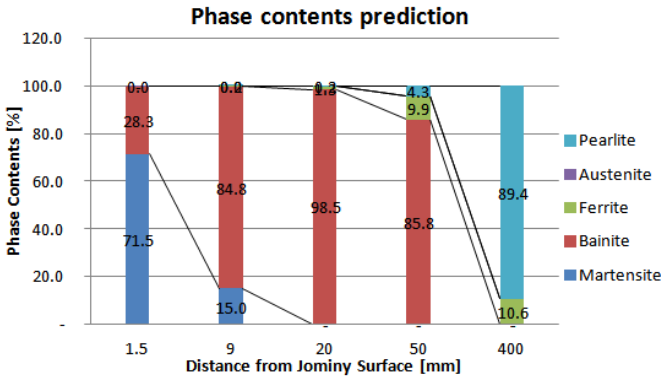

Figure 10: Phase content calculation of microstructure inspection position

Structural stability analysis considering mass effect

In the present study, the safety factor for load cases was calculated by using the main shaft drawing for a 5 MW wind power generator. The structural safety was evaluated in the case where the mechanical properties were constant over the entire specimen and in the case where strength was high in the surface region and low in the core due to the mass effect.

The structural safety was evaluated by using ANSYS 17.2 software, which is a commercial finite element analysis software package. The design feasibility was tested by calculating the stress and the safety factor for the cases where the torsional load of a 5 MW wind power generator and the bending load of the blades were applied simultaneously.

The main shaft of a wind power generator having an open structure [9] was employed as the main shaft model. In the design concept, the main shaft model includes a rotational shaft transmitting the torsional torque and a fixed shaft supporting the bending moment by the self-weight of the blades. Figure 11 shows the structural modeling, mesh system, and boundary conditions for the finite element analysis.

Torsional torque by the rotation of the rotor and bending moment by the self-weight of the blades are simultaneously applied to the main shaft. The torsional torque was calculated by using Equation (1), where P denotes the power (KW) and

R denotes the revolutions per minute (RMP):

$$T = 9549.3\frac{P}{R} = 9549.3\frac{5000}{12} = 3.98\times10^{9}[Nmm] \quad (1)$$

The bending moment was calculated by using the general equation for a MW turbine.

$$M = 13.412x^{2} + 75.91x = 7.148\times10^{8}[Nmm] \quad (2)$$

Figure 12 shows the equivalent stress obtained from the finite element analysis.

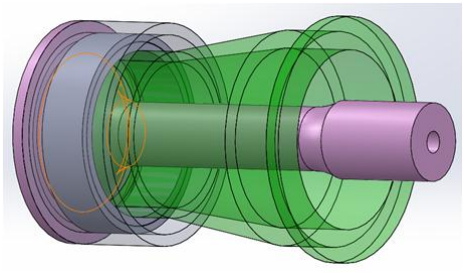

(a) Main Shaft assembly

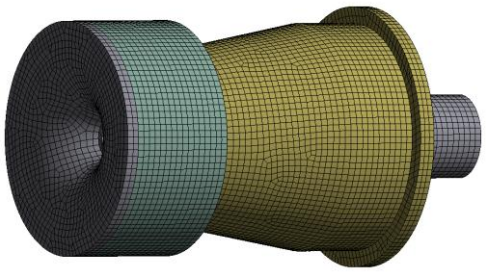

(b) Mesh System'

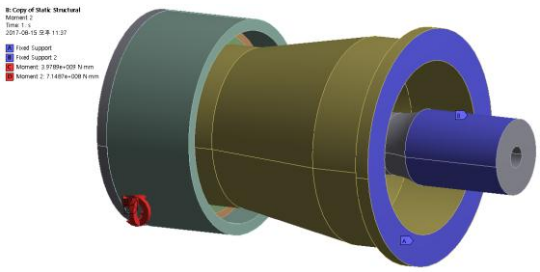

(c) Boundary conditions

Figure 11: Preprocessing of Finite Element Analysis

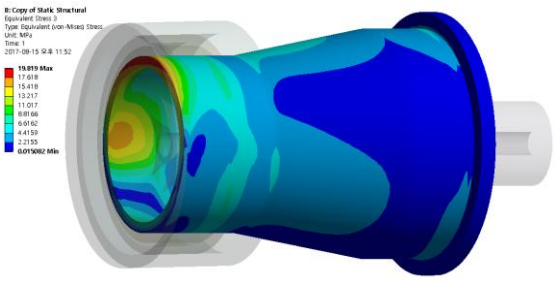

(a) Fixed Shaft

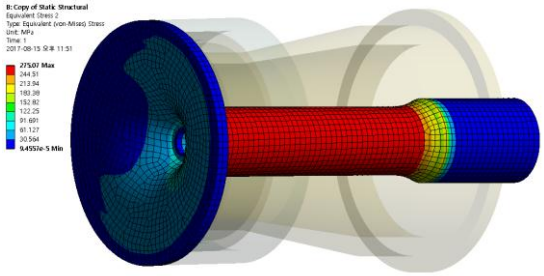

(b) Rotating Shaft

Figure 12: Equivalent stress of Main Shafts

According to EN10083, when the yield strength of 42CrMo4 is 550 MPa, the safety factors for the two main shafts are 2.0 and 27.7, respectively, as shown in Table 2.

Table 2: Safety factor on constant mechanical property conditions

Part Name	Equivalent Stress [MPa]	Yield Stress [MPa]	Safety Factor
Rotating Shaft	275.07	550	2.0
Fixed Shaft	19.8	550	27.7

The interval where the safety factor was lowest was the Φ520 interval for transmitting the torsional torque denoted by red color in Figure 12 (b). The safety factor was increased as the position was moved toward the core. Because the effective diameter was Φ520, the strength at individual positions could be predicted by using the hardness measurements obtained from the experiment performed by considering the mass effect. The relation between the hardness and the strength then may be substituted to express the tensile strength as a function of the depth. Finally, for the case where the ratio of the tensile strength is 68% of the yield strength, the mechanical properties could be expressed as a function of the depth.

However, since the yield strength should be compared with reference to a contrast yield condition of YS 550 MPa, the yield strength at 1/2", which is the EN10083 specimen position, was set to be 550 MPa, and the correlations among

the hardness, tensile strength, and yield strength may be expressed as given in the following equations. The hardness was calculated with reference to the hardness plot after the tempering of the surface region (S), because the cooling rate was high as the thickness was 170 mm at the outer diameter of Φ520 and the inner diameter of Φ180.

$$H_R C = 0.5865x^2 - 13.342x + 816.76 \quad (4)$$

$$TS = 0.4652x^2 - 10.584x + 647.96 \quad (5)$$

$$YS = 0.68TS \quad (6)$$

Figure 13 shows the plots representing the correlations of Equations (3) to (5), indicating that the hardness and the strength were highest on the cooling surface and decreased as the measurement position approached the core. However, the gradient of the strength reduction was decreased from 50 mm.

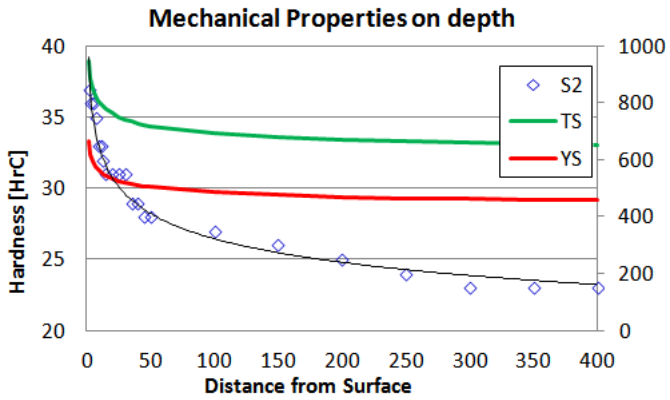

Figure 13: Mechanical Properties on Mass Effect Conditions

Since the YS value was dependent on the depth from the surface, if the YS relation shown above is applied, the safety factor in the Φ520 interval where the safety factor is the smallest is increased to 1/2" from the surface and then decreased moving toward the core. Figure 14 shows the safety factors calculated by considering the mass effect.

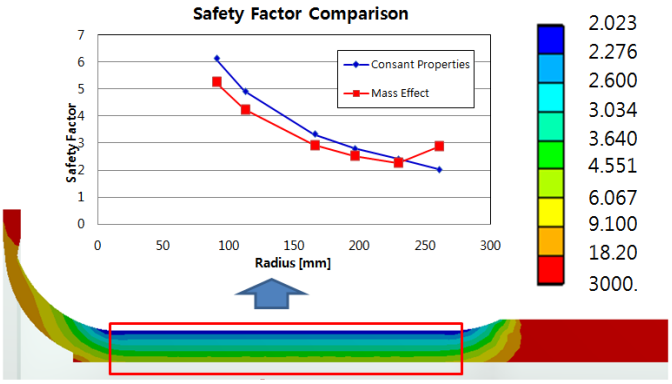

Figure 14: Safety factor comparison between constant mechanical properties and mass effect conditions

CONCLUSION

The main shaft for wind power generators is the heaviest part in the nacelle and is significantly affected by the mass effect due to its high weight. The mass effect should be quantified to secure structural safety of large-sized parts. In the present study, the Jominy test was performed with a large-sized specimen, and the hardness was measured and the microstructure was measured at different positions. Experimental results obtained from specimens of different sizes may not be applied to different specimens, an analytical method for analyzing the hardness depending on the weight, size, and cooling method is required. The hardness and the microstructure content obtained through the analyses using the DEFORM and JMatPro software programs were consistent with the values obtained from the experiment. However, since the hardness was excessively underestimated when the measurement point was close to the core, further studies are necessary. As the mass effect was quantified, the safety factor of the main shaft could be calculated by obtaining the yield strength depending on the depth from the surface. The hardness and the strength were expressed as functions of the depth from the surface by comparing the experimental results with the analytical results. In addition, to calculate the safety factor, the stress applied to the main shaft was analyzed through a finite element analysis. The safety factor calculated by considering the mass effect was higher in the surface region but lower in the core in comparison with the case where the strength of the entire specimen was constant. This verified that the calculation of the safety factor with consideration of the mass effect is a more stable and effective method for the main shaft structure.

ACKNOWLEDGEMENT

This study was performed as part of "Development of manufacturing technologies of Main shaft of 4MW class offshore wind turbine for asia market expansion" under the Energy Technology Development Project (20153030023920).

REFERENCES

[1] Wei Tong, 2010, Wind power generation and wind turbine design, WIT press, Billerica, USA

[2] YC Kwon, JH Kang, SS Kim, " Study on Manufacturing Process of Hollow Main Shaft by Open Die Forging", Transaction of Korean Society of Mechanical Engineers. A, Vol.40, No.2, pp221~227, 2016,

[3] DG Song, JH Kang, HW Lee, " A Study on Design of a Lightweight 7MW Class Offshore Wind-turbine Hollow Rotor Shaft", International Journal of Applied

Engineering Research, Vol.11, No.10, pp 7182~7187, 2016

[4] Steels for quenching and tempering - Part 3: Technical delivery conditions for alloy steels, 2007, EN10083

[5] Charlie R. Brooks, "Principles of the Heat Treatment of Plain Carbon and Low Alloy Steel", 1996, ASM International

[6] Structural steels with specified hardenability bands ", 2008, JIS G4052

[7] "Standrad Test Methods for Determining Hardenability of Steel", ASTM A 255

[8] S. Mitsuru, T. Ikuo, S. Junichi and S. Takashi, " Development of 5-MW Offshore Wind Turbine and 2-MW Floating Offshore Wind Turbine Technology", Hitach Review, Vol.63, pp414~421, 2014